ACS OMEGA

http://pubs.acs.org/journal/acsodf

Article

Benzothiazole Amides as TRPC3/6 Inhibitors for Gastric Cancer Treatment

Yingjie Wei,[▽] Mengxian Zhang,[▽] Zhenbin Lyu,[▽] Guolin Yang, Tian Tian, Mingmin Ding, Xiaodong Zeng, Fuchun Xu, Pengyu Wang, Fangfang Li, Yixuan Liu, Zhengyu Cao, Jing Lu,* Xuechuan Hong,* and Hongbo Wang*

Cite This: *ACS Omega* 2021, 6, 9196−9203

Read Online

ACCESS | Metrics & More | Article Recommendations | Supporting Information

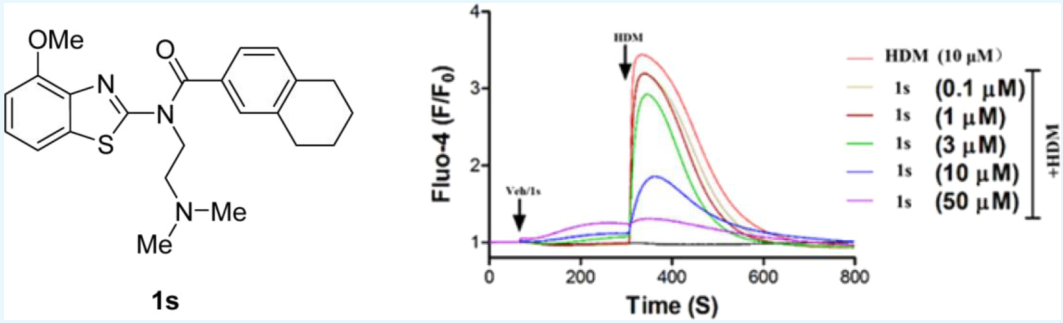

ABSTRACT: Transient receptor potential canonical channel 6 (TRPC6) has been implicated in many kinds of malignant tumors, but very few potent TRPC6 antagonists are available. In this study, a benzothiazole amide derivative **1a** was discovered as a TRPC6 activator in a cell-based high-throughput screening. A series of benzothiazole amide derivatives were designed and synthesized. The docking analyses indicated that the conformations of the compounds bound to TRPC6 determined the agonistic or antagonistic activity of the compounds against TRPC6, and compound **1s** with the tetrahydronaphthalene group in R_1 position fit well into the binding pocket of the antagonist-bound conformation of TRPC6. Compound **1s** showed an inhibitory potency order of TRPC3 (IC_{50} 3.3 ± 0.13 μM) ≈ C6 (IC_{50} 4.2 ± 0.1 μM) > C7 with good anti-gastric cancer activity in a micromolecular range against AGS and MKN-45, respectively. In addition, **1s** inhibited the invasion and migration of MKN-45 cells *in vitro*.

1. INTRODUCTION

Transient receptor potential canonical (TRPC) channels, which belong to the TRP family, are nonselective Ca^{2+} permeable cation channels expressed in various tissues.[1−5] Based on the amino acid sequence, TRPCs are grouped into TRPC1, TRPC2, TRPC3/6/7, and TRPC4/5 in which the TRPC3/6/7 shares 65−78% sequence identity.[4,6] TRPC6 has been reported to involve the regulation of cardiac hypertrophy, pulmonary vascular tone and permeability, blood pressure, renal fibrosis, and Alzheimer's disease.[7−13] TRPC6 also plays a key role in the carcinogenesis and is overexpressed in gastric cancer, breast cancer, and glioblastoma. However, only a low level of TRPC6 is expressed in the corresponding gastric normal tissues, indicating that TRPC6 channels might be a novel anti-cancer drug target against gastric cancer.[14−18]

Due to the high sequence conservation among TRPCs, it is very challenging to design selective small-molecule TRPC6 antagonists. Very few compounds have been reported as TRPC6 inhibitors.[5,11,19−25] 1*H*-Imidazole, 1-[2-(4-methoxyphenyl)-2-[3-(4-methoxyphenyl)propoxy]ethyl] (**SKF-96365**), a nonselective TRPC6 antagonist with an IC_{50} value of 4.9 μM has been reported to inhibit the Ca^{2+} elevation regulated by TRPC6 channels.[14,26,27] The IC_{50} values of specific TRPC6 antagonists, 2-(phenylamino)thiazol-4-yl)-(piperidin-1-yl)methanone derivatives (**SAR-7334**, Figure 1), [4-(6-aminopyridazin-3-yl)piperidin-1-yl]-[4-[4-(trifluoromethy-l)phenoxy] phenyl]methanone (**BI 749327**), 4-(((1*R*,2*R*,3a*R*,7a*S*)-2-((*R*)-3-aminopiperidin-1-yl)-3a,7a-dimethyl-5-oxooctahydro-1*H*-inden-1-yl)oxy)benzonitrile (**DS88790512**), and larixol congener **SH045** were 7.9, 13, 11, and 5.8 nM, respectively.[11,28−31] Although a number of TRPC6 antagonists were reported in a nanomolar range, very few of them were utilized *in vivo*, partially due to the low potency and poor bioavailability.[11] Our group has reported a selective TRPC3 agonist **HDM** with the pyrazolopyrimidine skeleton, demonstrating high affinity with EC_{50} (TRPC3) ∼19

Received: January 28, 2021
Accepted: March 16, 2021
Published: March 24, 2021

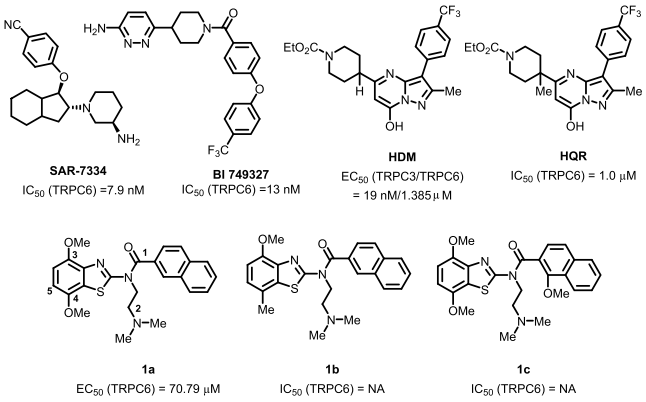

Figure 1. Active compounds targeted TRPC6.

nM and EC_{50} (TRPC6) ~1.385 μM.[32] One methyl group was added into **HDM** to produce a high selective TRPC6 antagonist **HQR** with an IC_{50} value of ~1 μM, which suppressed the gastric cancer cells proliferation and the growth of xenograft tumors.[33]

A variety of benzothiazole amides analogs from the Molecular Libraries Small Molecule Repository (MLSMR) were screened using the fluorescence Ca^{2+} assay. Compound **1a** (PubChem: 24761863, Figure 1) was first founded as a TRPC6 agonist with an EC_{50} value of ~70.79 μM as the primary hit. The replacement of methoxyl group with methyl group (**1b**) at position 4 and 1-methoxyl substitution of the naphthalene at position 1 (**1c**) led to the loss of agonist activity of the source lead compound, suggesting that the substitution at position 1 or 4 may play an important role in the structure−activity relationship study.

2. RESULTS AND DISCUSSION

2.1. Rational Design. Subtle difference in the compound structure induces the activity alternation, which may attribute to the different binding modes of the compounds against the antagonist-bound or agonist-bound conformation of TRPC6. The mutation of Glu509 on S2 and Asp530 on S3 almost completely abolished the response of TRPC6 to the antagonist **AM-1473**, and the side chains of His446 on S1 and Arg758 on the reentrant loop moved for adapting to the antagonist-binding (PDB: 6uza) compared to no major structural changes in the side chains of agonist-bound conformation (PDB: 6uz8),[31] which characterized the important roles of these residues bound to the antagonists. Molecular docking analyses were carried out to analyze the difference between the antagonists and agonists against TRPC6. In the case of **SAR-7334** and **BI 749327**, the TRPC6 inhibitory activities could be explained by the possible interactions between the compounds and the antagonist-bound conformation of TRPC6. **SAR-7334** and **BI 749327** fit much deeper into the residues of S1-S4, the TRP helix and the membrane-reentrant loop, which formed the basis for the inhibitory study (Figure S1). **SAR-7334** engaged in one hydrogen-bond interaction with Glu509 and one van der Waals contact with Asp530 (Figure 2A). Moreover, **SAR-7334** was involved one $\pi-\pi$ interaction with His446 as well as one π-cation with Arg758. **BI 749327** made a hydrogen-bond interaction with Glu509, a π-alkyl interaction with His446 and a weak van der Waals contact with Arg758 (Figure 2B), which may explain the decreased antagonistic effect of **BI 749327**. However, the agonists **HDM** and **1a** lacked intermolecular interactions with these key residues and

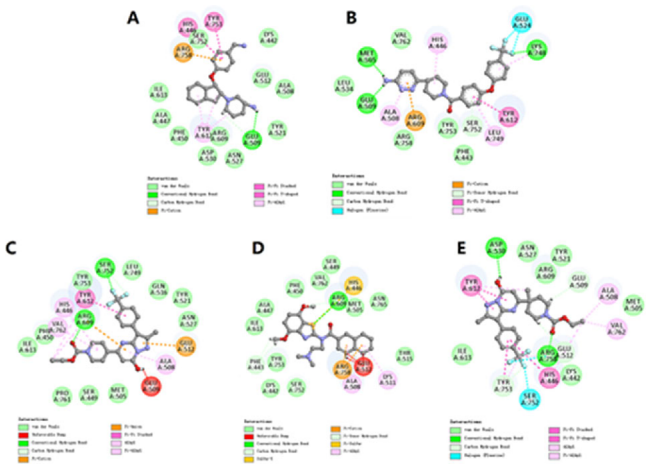

Figure 2. Detailed interactions of **SAR-7334** (A), **BI 749327** (B), **HDM** (C), **1a** (D), and **HQR** (E) interacted with the antagonist-bound conformation of TRPC6 (PDB ID: 6uza). The 3D binding modes of TRPC6 and the compounds are shown in Figure S1.

even formed unfavorable bumps with the residues of TRPC6 (Figure 2C,D), which induced the loss of antagonistic activities of these two compounds.

HDM had the agonistic activity against TRPC6 (EC_{50} = 1.385 μM), and its methylated derivative (**HQR**) showed moderate antagonistic activity against TRPC6 (IC_{50} = 1.0 μM). The docking analyses indicated that the methyl group induced the conformational change of **HQR** by producing the steric effect and fit well into the antagonist-bound conformation of TRPC6 (Figure S1), which was similar with **SAR-7334** and **BI 749327**. **HQR** formed a hydrogen bond with Asp530 and a weak van der Waals contact with Glu509 (Figure 2E). This indicated that the conformations of the compounds bound to TRPC6 determined the agonistic or antagonistic activity of the compounds against TRPC6.

2.2. Structure−Activity Relationship (SAR) Analysis. Based on the activity alteration from **HDM** to **HQR**, the possibility of converting the agonist **1a** into an antagonist was explored. Benzothiazole amides **1d-1af** by further diversification of **1a** at position R_1-R_5 were designed, synthesized, and evaluated in the HEK293 cellular assay system with a stable expression of the mouse TRPC6.

A series of compounds were first designed and synthesized through rational drug design and structure−activity relationship. Compounds **1d-1v** containing 4-methoxyben-zo[*d*]-thiazol-2-yl heterocycle with various aromatic substituents and 4-dialkylamino substituents at position R_1 and R_2 were synthesized and evaluated, respectively. No *in vitro* potency was observed when the 2-chloro-5-thiophene group at position R_1 replaced with 2-methoxypyridin-4-yl (**1d-1g**), styrene (**1h-1k**) or 2-naphthalene (**1r**, **1t-1v**, Table 1). Surprisingly, incorporation of 4-(trifluoromethyl) benzene (**1m-1o**), benzo-[d][1,3]dioxole (**1p-1q**) at position R_1 with the dialkylamino group at position R_2 (**1m-1q**) resulted in analogs with the TRPC6 inhibitory potency. The steady increase in potency of the described compounds (**1o** > **1n** > **1m** > **1l**, **1q** > **1p**) was identified by the introduction of a larger size of the amino substituents at position R_2 from dimethylamino, diethylamino, 1-pyrrolidine to 1-piperidine group. It is interesting that the naphthalene group in compound **1r** was replaced with 1,2,3,4-tetrahydronaphthalene group (**1s**), resulting in the improved antagonistic activity of **1s** against TRPC6 (IC_{50} = 4.2 ± 0.1

https://doi.org/10.1021/acsomega.1c00514
ACS Omega 2021, 6, 9196−9203

Table 1. Inhibitory Effects of 1d-1v against TRPC6 Channels

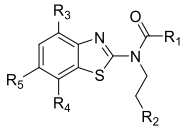

1d-1v: R_3 = OMe, R_4 = R_5 = H

Cpd	R_1	R_2	IC_{50} (μM)[a]	Cpd	R_1	R_2	IC_{50} (μM)[a]
1d			NA	1n			34.5 ± 0.5
1e			NA	1o			28.7 ± 0.6
1f			NA	1p			14.7 ± 0.2
1g			NA	1q			6.8 ± 0.2
1h			NA	1r			NA
1i			NA	1s			4.2 ± 0.1
1j			NA	1t			NA
1k			NA	1u			NA
1l			NA	1v			NA
1m			128.0 ± 0.3				

[a]Effects on the activity of TRPC6 or the IC_{50} value against the activity of TRPC6 activated by the **HDM** at a concentration of 10 μM,[32] which was calculated based on one experiment (N = 3); NA: No activity.

μM by Ca^{2+} assay). Therefore, the binding modes of **1r** and **1s** interacted with the TRPC6 were further analyzed for explaining the activity alteration.

The compounds with the naphthalene substituents at position R_1 (**1a-1c, 1r, 1t-1v**) had no antagonistic potency against TRPC6. The naphthalene group in **1a** formed an unfavorable bump with Glu512 in the antagonist-bound conformation of TRPC6 by docking analyses. The demethoxy derivative (**1r**) also showed similar conformation against TRPC6 (Figure 3A,C). Therefore, we hypothesized that the

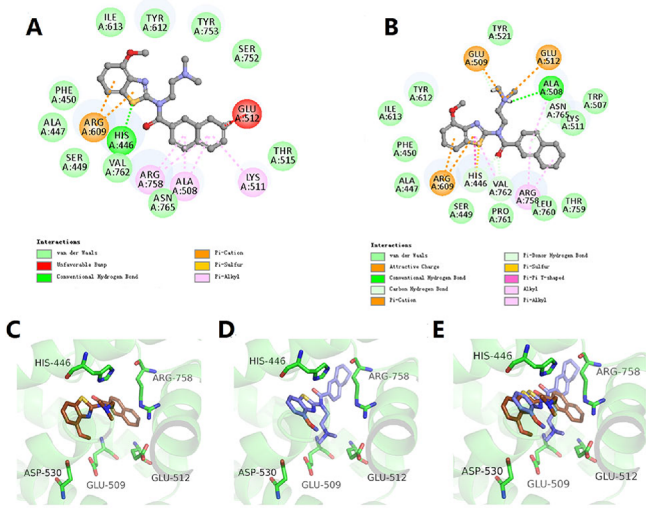

Figure 3. The binding modes of **1r** (A, C) and **1s** (B, D) interacted with the antagonist-bound conformation of TRPC6 (PDB: 6uza). **1r** and **1s** were shown in brown and blue sticks in 3D mode. (E) Superimposed docking structures of TRPC6 in complex with **1s** and **1r**.

naphthalene group may not be an optimal design, and the group should be substituted to reduce the unfavorable bump with the target. The naphthalene group was replaced with the tetrahydronaphthalene (**1s**), which made a distortion in this position, alternated the stacking angle, and eliminated unfavorable bumps. Moreover, the *N*,*N*-dimethylamino ethyl moiety of **1s** had polar interactions with Glu509 and Glu512, respectively (Figure 3B,D), and the benzo[*d*]thiazole core of **1s** was involved in a π-cation interaction with Arg609, confirming the stable binding pattern *in vitro* assay.

Based on the characteristics of the metal ion in the TRPC6 channel, we tried to introduce sulfur atoms and designed a series of compounds. The importance of the substitution at the R_2 position of the benzothiazole ring on the activity of TRPC6 was explored with compounds **1w-1ab**. When R_1 was 2-chloro-5-thiophene, benzothiazole amides **1w-1ab** demonstrated varying levels of antagonist activity against TRPC6 (Table 2). Without the methoxyl substitution at position R_3−R_5 on the phenyl ring has led to analogs **1aa-1ab** with good antagonist potency at the TRPC6 receptor with a mean IC_{50} value of 15.1 ± 1.4 and 8.8 ± 1.3 μM, respectively. The potency of the dimethyl amino group (**1w**, **1y**, and **1aa**) at position R_2 was ∼2−4 folds lower than that of the prototypical pyrrolidine substituent (**1x**, **1z**, and **1ab**). However, the 2-bromo-5-thiophene group at position R_1 had a deleterious effect on the TRPC6 antagonist potency (**1 ac-1ad**) as did the 2-bromo-5-furan group at position R_1 (**1ae-1af**).

2.3. Functional Characterization of 1s on the Activities of TRPC3-TRPC7. Compound **1s** inhibited the $[Ca^{2+}]_i$ increases evoked **by HDM** (10 μM) with an IC_{50} value of 4.2 ± 0.1 μM in TRPC6-expressing cells (n = 3) (Figure

https://doi.org/10.1021/acsomega.1c00514
ACS Omega 2021, 6, 9196−9203

Table 2. Effect of Compounds 1w−1af on TRPC6 Channels

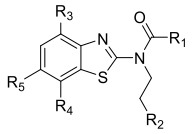

1w-1af

Cpd	R_1	R_2	R_3	R_4	R_5	IC_{50} (μM)[a]
1w			MeO	H	H	138.9 ± 6.4
1x			MeO	H	H	63.9 ± 0.4
1y			H	H	MeO	61.1 ± 5.4
1z			H	H	MeO	33.0 ± 1.9
1aa			H	H	H	15.1 ± 1.4
1ab			H	H	H	8.8 ± 1.3
1ac			MeO	H	H	NA
1ad			MeO	H	H	NA
1ae			MeO	H	H	NA
1af			MeO	H	H	NA

[a]Effects on the activity of TRPC6 or the IC_{50} value against the activity of TRPC6 activated by the **HDM** at a concentration of 10 μM,[32] which was calculated based on one experiment (N = 3); NA: No activity.

4A,B) without self-fluorescence, and **1s** was chosen to further explore. **1s** immediately suppressed the TRPC6 currents evoked by the **GSK1702934A** (1 μM) in the whole-cell voltage clamp assay (Figure 4C). Based on the currents at +80 mV, an IC_{50} value of **1s** for the monovalent cation currents of TRPC6 was calculated as 4.19 ± 0.04 μM (Figure 4D, n = 6−8), which was comparable to that obtained in the Ca^{2+} assay (Table 1).

The effect of **1s** on the TRPC3 and TRPC7 channels was examined by the fluorescence Ca^{2+} assay. Similar as TRPC6, **1s** caused a detectable change in intracellular Ca^{2+} concentration ($[Ca^{2+}]_i$) in TRPC3-HEK293 cells in a concentration-dependent manner (Figure 5A,E). Treatment with **1s** inhibited the response to subsequent application of **HDM** (10 μM), obtaining the IC_{50} values of 3.3 ± 0.13 μM (Figure 5B). Different from TRPC3/6, **1s** almost did not cause a discernible Ca^{2+} response in TRPC7-HEK293 cells (Figure 5F). These data indicate that **1s** is an effective antagonist of TRPC3/6 channels, and its potency order is TRPC3 ≈ C6 > C7.

The above data indicate that the benzothiazole amide **1s** has antagonistic activity on the TRPC3/6 subgroup of TRPC channels. To verify the selectivity, the Ca^{2+} assay was used to detect the effects of **1s** on stable HEK293 cell line that co-expressed TRPC4/5 and μ-opioid receptor and on HEK293 cell lines expressing TRPA1, TRPM8, TRPV1, and TRPV3.

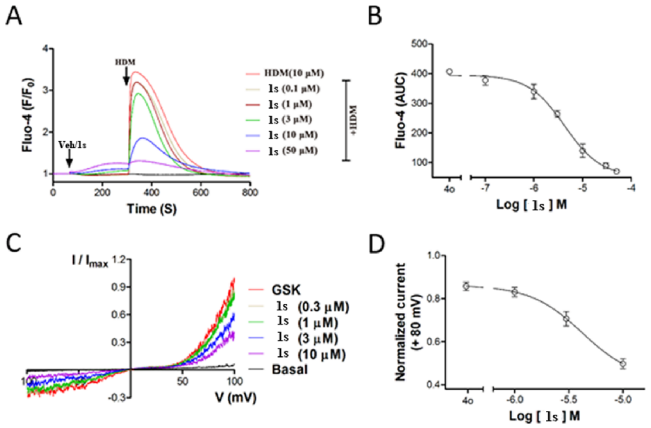

Figure 4. Compound **1s** inhibited TRPC6 expressed in HEK293 cells. (A) **1s** inhibited the Ca^{2+} response in TRPC6-HEK293 cells induced by **HDM**. Inoculated cells in the 96-well plate were loaded with Fluo-4, and fluorescence changes were read in a microplate reader while adding **1s** and **HDM**, as shown by horizontal bars at the top of the traces. The traces represent the reading (F_0) of three repeated measurements of an experiment at the beginning, normalized to the average fluorescence changes (ΔF) of fluorescence, which was repeated three times. (B) Concentration-response curves for compound **1s** inhibiting TRPC6 was determined by Ca^{2+} assay (Fluo-4). The solid lines indicated the fitting of the Hill equation, which obtained the IC_{50} values. (C) By changing the concentration of compound **1s** in the TRPC6 cell, the current−voltage (I−V) relationships were acquired through the voltage ramps. **GSK1702934A** (1 μM) activated current and **1s** inhibited current. (D) Concentration-response curves for compound **1s** determined by electrophysiology recording to inhibit TRPC6. The solid lines were represented by the Hill equation, which produced the IC_{50} value.

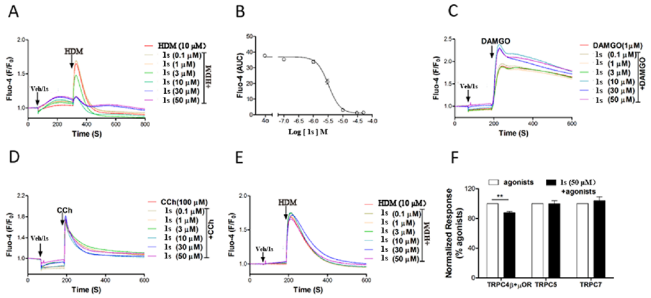

Figure 5. Compound **1s** inhibited agonist-evoked TRPC3/4/5/7 activity. **1s** inhibited the increase of $[Ca^{2+}]_i$ in HEK293 cells that expressed human TRPC3 (A, induced by 10 μM **HDM**), mouse TRPC4 (C, induced by 1 μM **DAMGO**), mouse TRPC5 (D, induced by 100 μM **CCh**), and mouse TRPC7 (E, induced by 10 μM **HDM**). (B) Concentration-response curves for compound **1s** inhibiting TRPC3 was determined by Ca^{2+} assay (Fluo-4). (F) Compound **1s** had little or no effect on Ca^{2+} response in TRPC7-HEK293 cells.

For TRPC4, **1s** only partially inhibited the membrane depolarization induced by **DAMGO** (1 μM), indicating a very weak inhibitory activity (Figure 5C). For TRPC5-, TRPA1-, TRPM8-, TRPV1-, and TRPV3-expressing cells planted in 96-well plates and wells loaded with Fluo-8, **1s** (50 μM) did not significantly affect the Ca^{2+} response induced by the agonist of the corresponding channels (Figure 5D). Therefore, compound **1s** significantly inhibited TRPC3/6, had a weak effect on TRPC4, and no effect on TRPC5 and other TRP channels.

https://doi.org/10.1021/acsomega.1c00514
ACS Omega 2021, 6, 9196−9203

2.4. Anti-Proliferation Activity of 1s against Gastric Cancer Cells *in vitro*. The anti-gastric cancer activity of compound **1s** was tested with **SKF-96365** as a positive control. **1s** exhibited remarkable cytotoxicity against the two human gastric cancer cell lines. It inhibited cell proliferation of both MKN-45 and AGS in a dose-dependent manner, with IC_{50} values of 8.00 ± 0.51 and 12.03 ± 1.01 μM, respectively, which was better than **SKF-96365** with the IC_{50} values of 15.34 and 37.03 μM in the same condition (Figure 6).

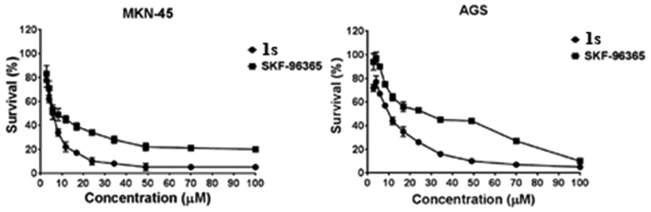

Figure 6. Cytotoxicity of **1s** against MKN-45and AGS cells. MKN-45 or AGS cells were treated with the indicated concentrations of compound **1s** or **SKF-96365** for 72 h, and then the cell viability was detected by the MTT assay. Data were normalized to the same trial without drug treatment and to the means ± SEM of the three trials.

2.5. Anti-Cell Migration and Invasion of 1s against MKN-45 Cells. The wound-healing migration assay and Boyden chamber assay were applied to evaluate the effect of **1s** on the migration and invasion of MKN-45 cells. Treatment with **1s** at a concentration of 5 μM inhibited the MKN-45 cell migration (Figure 7A,C). At the same time, **1s** impaired the activity of MKN-45 cells to move through the pores toward the chemoattractant below (Figure 7B,D).

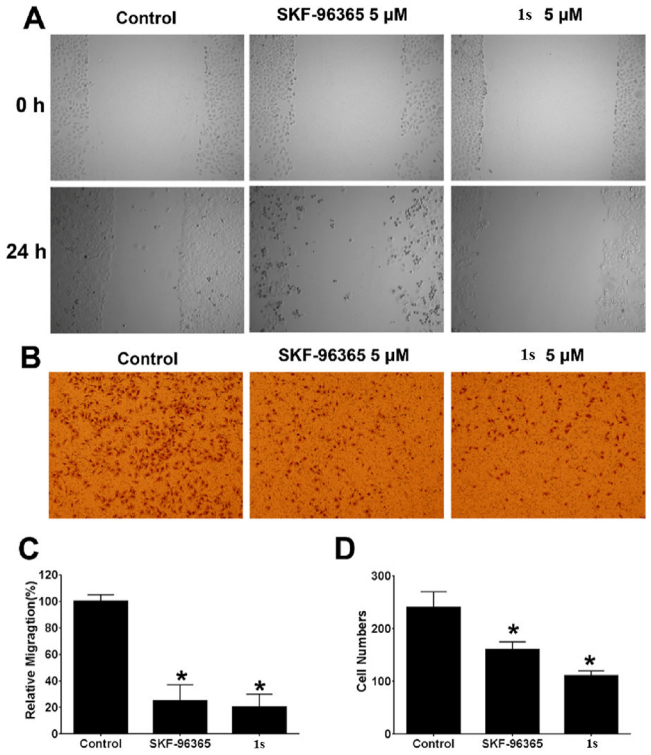

Figure 7. Compound **1s** inhibited the migration and invasion of MKN-45 cells. (A, C) MKN-45 cells were treated with **SKF-96365** and **1s** at the indicated concentrations. Scratches were made and images were taken at 0 and 24 h, and the migration distances were summarized. (B, D) MKN-45 cells in serum-free medium were plated at the top uncoated membranes with **SKF-96365** and **1s** at specified concentrations, and the lower chamber was filled with a complete medium and cells were then allowed to migrate for 24 h, and the cells on the bottom part of the membrane were stained with crystal violet and summarized. *$p < 0.05$, compared with the control group.

3. CONCLUSIONS

In summary, the pharmacological properties of newly synthesized benzothiazole amides compounds as novel TRPC3/6 antagonists were studied by $[Ca^{2+}]_i$-imaging and electrophysiology recording. A lead compound **1a** was identified as a TRPC6 activator with an EC_{50} of ∼70.79 μM as a starting point. Chemical modifications on the benzothiazole amide scaffold focused on the introduction of aromatic groups at R_1 and amino groups at R_2. Twenty-nine benzothiazole amides were designed and synthesized. Compound **1s** has an IC_{50} value of 4.2 ± 0.1 μM in TRPC6-expressing cells. Compared with other TRP families, **1s** has a reasonable selective high potency against TRPC3/6 and has no effect on the TRPC5, TRPC7, and other TRP channels. Furthermore, compound **1s** has a strong inhibition effect on the activation of TRPC6 mediated by **HDM** and has an inhibitory effect on the proliferation of gastric cancer cells, MKN-45, and AGS cells with the IC_{50} values of 8.00 ± 0.51 and 12.03 ± 1.01 μM, respectively. Further experiments are currently underway to evaluate its pharmacokinetic profile, *in vivo* anti-tumor activity as well as its mechanism of anti-gastric cancer activity and potential therapeutic utilities, and the results will be reported in the near future.

4. EXPERIMENTAL SECTION

4.1. General Methods. All commercially available starting materials and solvents were reagent grade and used without further purification. Unless otherwise specified, all reactions were performed under an argon atmosphere. The reaction progress was monitored by thin-layer chromatography (TLC). The purification of all compounds was purified by silica gel column chromatography. ^1H and ^{13}C NMR spectra were recorded on a Bruker AV400 spectrometer (^1H-400 MHz, ^{13}C-101 MHz). High-resolution mass spectrometry (HRMS) was performed with a Thermo LTQ XL Orbitrap instrument. Low-resolution mass spectrometry (ESI-MS) was performed on AB Sciex 4000 Qtrap.

4.2. Synthesis. The synthesis route (Scheme S1) and NMR spectra of benzothiazole amides derivatives **3d-7af** are provided in the Supporting Information.

4.3. Channel Inhibition. Antagonism of synthesized TRPC6 ligands were evaluated *in vitro*, as measured by inhibition of receptor activation by the TRPC6 agonist **HDM** as previously reported.[32] The human embryonic kidney HEK293 cell line that co-expressed mouse TRPC6 and the $G_{q/11}$-PLC-coupled M5 muscarinic receptor was detected by fluorometric assay. These cells showed a strong persistent membrane depolarization respond to the muscarinic agonist, carbachol (**CCh**), which could be detected by the FLIPR membrane potential (FMP) dye as an increase in fluorescence. In transfected HEK293 cells, the tested compounds did not significantly activate the TRPC6-mediated Ca^{2+} increase. On the other hand, the TRPC6-HEK293 cells were preincubated with different doses of the tested compounds (5 min) and then incubated with the agonist **HDM** (10 μM), and Ca^{2+} elevation

https://doi.org/10.1021/acsomega.1c00514
ACS Omega 2021, 6, 9196−9203

in most cells was inhibited due to the response of TRPC6 to the agonist **HDM**.

4.4. Cell Viability Assay. The MTT detection method is based on our previous protocol.[33] Briefly, the cells (2000/well) were seeded into 96-well plates and incubated overnight and then treated with the tested compounds. After 72 h, the MTT solution was added and then incubated for 4 h. The MTT-formazan formed was dissolved in DMSO in which the absorbance was then measured at 570 nm with a microplate analyzer. The cell relative survival rate and the IC_{50} were calculated.

4.5. Wound Healing Assay. Following our previous protocol, the wound-healing assay was used to evaluate cell migration.[33] Briefly, MKN-45 cells were seeded in a 24-well plate and cultured overnight. The wound was yielded by scraping with a sterile 200 μL pipette tip and treated it with the specified concentrations of tested compounds. After 0 and 24 h, images of the wound distance were quantified via measuring the width of the cell-free zone at six distinct positions with a digitally calibrated micrometer by microphotographs with an OLYMPUS IX 73 inverted microscope equipped with a CCD camera, and the relative migration distance was calculated using Image J software.

4.6. Transwell Cell Migration Assays. Transwell migration assays were performed using 6-well Transwell chambers (Corning Life Sciences, Lowell, MA, USA) containing 8 μm permeable pores according to the manufacturer's instructions. The cells cultured in the serum-free medium were seeded at the top uncoated membranes with the tested compounds, and the lower chamber was filled with a complete medium containing 10% FBS. The cells were allowed to migrate for 24 h, and the cells in the upper surface of the membrane were carefully washed using PBS and removed with a cotton swab. After that, the cells on the bottom part of the membrane were fixed and stained with crystal violet in which the cells were visualized and counted from six randomly selected fields using fluorescent inverted microscope. Directional migration was quantified by cell counting using Image J.

4.7. Molecular Docking. The crystal structures of hTRPC6 in complex with **AM-1473** (PDB: 6UZA and 6UZ8) was used as the receptors for docking-based studies. The geometry of proteins was first optimized with Dreiding-like force field and subsequently run through the "clean protein" from macromolecular module in Discovery Studio 2018 toolbox to standardize a detailed check. After preparing the protein complexes by monitoring the bad valence, removing all water molecules and adding hydrogens, CHARMm force field was applied to the receptors and the benzothiazole amides. The active site spheres centered on its cognate ligand was created with an automatic generated diameter of 10 Å. The remained parameters were referred to keep default settings.

4.8. Statistical Analysis. Data are expressed as the mean ± SEM. The analysis of the data obtained from *in vitro* experiments was performed using Origin 7.5 (Origin Lab) and GraphPad Prism (V 5.01). Statistically significant differences between two sets of data were evaluated with the Student's *t*-test ($p < 0.05$). Statistical comparisons between multiple (>3) experimental groups were performed with analysis of variance (ANOVA) and Student's *t*-test. Values with a $p < 0.05$ were considered statistically significant.

■ ASSOCIATED CONTENT

Supporting Information

The Supporting Information is available free of charge at https://pubs.acs.org/doi/10.1021/acsomega.1c00514.

Chemistry of **1d-1af**, the synthesis route of **3d-7af**, docking modes of the compounds interacted with the antagonist-bound conformation of TRPC6, ^{1}H and ^{13}C NMR of 1d-1af, and HRMS of 1d-1af (PDF)

■ AUTHOR INFORMATION

Corresponding Authors

Jing Lu − *School of Pharmacy, Key Laboratory of Molecular Pharmacology and Drug Evaluation (Yantai University), Ministry of Education; Collaborative Innovation Center of Advanced Drug Delivery System and Biotech Drugs in Universities of Shandong, Yantai University, Yantai 264005, China; State Key Laboratory of Long-acting Targeting Drug Delivery Technologies, Luye Pharma Group Ltd., Yantai 264003, China;* orcid.org/0000-0001-9195-7470; Email: lujing_ytu@126.com

Xuechuan Hong − *State Key Laboratory of Virology, College of Science, Research Center for Ecology, Laboratory of Extreme Environmental Biological Resources and Adaptive Evolution, Innovation Center for Traditional Tibetan Medicine Modernization and Quality Control, Tibet University, Lhasa 850000, China; Key Laboratory of Combinatorial Biosynthesis and Drug Discovery (MOE) and Hubei Province Engineering and Technology Research Center for Fluorinated Pharmaceuticals, Wuhan University School of Pharmaceutical Sciences, Wuhan 430071, China; Shenzhen Institute of Wuhan University, Shenzhen 518057, China;* Email: xhy78@whu.edu.cn

Hongbo Wang − *School of Pharmacy, Key Laboratory of Molecular Pharmacology and Drug Evaluation (Yantai University), Ministry of Education; Collaborative Innovation Center of Advanced Drug Delivery System and Biotech Drugs in Universities of Shandong, Yantai University, Yantai 264005, China*; Email: hongbowangyt@ytu.edu.cn

Authors

Yingjie Wei − *School of Pharmacy, Key Laboratory of Molecular Pharmacology and Drug Evaluation (Yantai University), Ministry of Education; Collaborative Innovation Center of Advanced Drug Delivery System and Biotech Drugs in Universities of Shandong, Yantai University, Yantai 264005, China*

Mengxian Zhang − *Key Laboratory of Combinatorial Biosynthesis and Drug Discovery (MOE) and Hubei Province Engineering and Technology Research Center for Fluorinated Pharmaceuticals, Wuhan University School of Pharmaceutical Sciences, Wuhan 430071, China*

Zhenbin Lyu − *State Key Laboratory of Virology, College of Science, Research Center for Ecology, Laboratory of Extreme Environmental Biological Resources and Adaptive Evolution, Innovation Center for Traditional Tibetan Medicine Modernization and Quality Control, Tibet University, Lhasa 850000, China*

Guolin Yang − *State Key Laboratory of Natural Medicines, Jiangsu Provincial Key Laboratory for TCM Evaluation and Translational Development, China Pharmaceutical University, Nanjing, Jiangsu Province 211198, China*

https://doi.org/10.1021/acsomega.1c00514
ACS Omega 2021, 6, 9196−9203

Tian Tian − *State Key Laboratory of Virology, College of Science, Research Center for Ecology, Laboratory of Extreme Environmental Biological Resources and Adaptive Evolution, Innovation Center for Traditional Tibetan Medicine Modernization and Quality Control, Tibet University, Lhasa 850000, China; Key Laboratory of Combinatorial Biosynthesis and Drug Discovery (MOE) and Hubei Province Engineering and Technology Research Center for Fluorinated Pharmaceuticals, Wuhan University School of Pharmaceutical Sciences, Wuhan 430071, China*

Mingmin Ding − *Key Laboratory of Combinatorial Biosynthesis and Drug Discovery (MOE) and Hubei Province Engineering and Technology Research Center for Fluorinated Pharmaceuticals, Wuhan University School of Pharmaceutical Sciences, Wuhan 430071, China*

Xiaodong Zeng − *Key Laboratory of Combinatorial Biosynthesis and Drug Discovery (MOE) and Hubei Province Engineering and Technology Research Center for Fluorinated Pharmaceuticals, Wuhan University School of Pharmaceutical Sciences, Wuhan 430071, China; Shenzhen Institute of Wuhan University, Shenzhen 518057, China*

Fuchun Xu − *State Key Laboratory of Virology, College of Science, Research Center for Ecology, Laboratory of Extreme Environmental Biological Resources and Adaptive Evolution, Innovation Center for Traditional Tibetan Medicine Modernization and Quality Control, Tibet University, Lhasa 850000, China*

Pengyu Wang − *Key Laboratory of Combinatorial Biosynthesis and Drug Discovery (MOE) and Hubei Province Engineering and Technology Research Center for Fluorinated Pharmaceuticals, Wuhan University School of Pharmaceutical Sciences, Wuhan 430071, China*

Fangfang Li − *School of Pharmacy, Key Laboratory of Molecular Pharmacology and Drug Evaluation (Yantai University), Ministry of Education; Collaborative Innovation Center of Advanced Drug Delivery System and Biotech Drugs in Universities of Shandong, Yantai University, Yantai 264005, China*

Yixuan Liu − *State Key Laboratory of Virology, College of Science, Research Center for Ecology, Laboratory of Extreme Environmental Biological Resources and Adaptive Evolution, Innovation Center for Traditional Tibetan Medicine Modernization and Quality Control, Tibet University, Lhasa 850000, China*

Zhengyu Cao − *State Key Laboratory of Natural Medicines, Jiangsu Provincial Key Laboratory for TCM Evaluation and Translational Development, China Pharmaceutical University, Nanjing, Jiangsu Province 211198, China*

Complete contact information is available at: https://pubs.acs.org/10.1021/acsomega.1c00514

Author Contributions

[▽]Y.W., M.Z., and Z.L. contributed equally to this work. Y.W. and F.L. performed the pharmacological experiments. M.Z. and Z.L. performed compound synthesis and optimization. T.T., M.D., X.Z., F.X., P.W., and Y.L. also contributed to compound synthesis. G.Y. and Z.C. performed the test on channel activity. J.L. performed molecular modeling. X.H. and H.W. designed the experimental idea and gave guidance. The manuscript was written through contributions of all authors. All of the authors approved the final version of the manuscript.

Notes

The authors declare no competing financial interest.

■ ACKNOWLEDGMENTS

This work was partially supported by grants from Key Research Project of Yantai (2019XDHZ102), National Natural Science Foundation of China (82073888, 81773674), the Science and Technology Support Program for Youth Innovation in Universities of Shandong (2019KJM009), Top Talents Program for One Case Discussion of Shandong Province, the National Key R&D Program of China (2020YFA0908800), Shenzhen Science and Technology Research Grant (JCYJ20190808152019182), Hubei Province Scientific and Technical Innovation Key Project (2020BAB058), the Applied Basic Research Program of Wuhan Municipal Bureau of Science and Technology (2019020701011429), the Local Development Funds of Science and Technology Department of Tibet (XZ202001YD0028C), and the Fundamental Research Funds for the Central Universities (ZNJC201931).

■ ABBREVIATIONS

$[Ca^{2+}]_i$, intracellular Ca^{2+} concentration; DAG, diacylglycerols; IPAc, isopropyl acetate; TFA, trifluoroacetic acid; DMAP, 4-dimethylaminopyridine; DMF, *N*,*N*-Dimethylformamide; EC_{50}, half maximal effective concentration; FMP, FLIPR Membrane potential; TRPC, transient receptor potential canonical; TRPV, transient receptor potential vanilloid; TRPM, transient receptor potential melastatin; SAR, structure−activity relationship; TRPA, transient receptor potential ankyrin; MLSMR, Molecular Libraries Small Molecule Repository; TLC, thin-layer chromatography; HRMS, high-resolution mass spectrometry; ESI-MS, low-resolution mass spectrometry

■ REFERENCES

(1) Ong, H. L.; de Souza, L. B.; Ambudkar, I. S. Role of TRPC Channels in Store-Operated Calcium Entry. *Adv. Exp. Med. Biol.* **2016**, *898*, 87−109.

(2) Hofmann, T.; Obukhov, A. G.; Schaefer, M.; Harteneck, C.; Gudermann, T.; Schultz, G. Direct activation of human TRPC6 and TRPC3 channels by diacylglycerol. *Nature* **1999**, *397*, 259−263.

(3) Zhang, H.; Liu, H.; Luo, X.; Wang, Y.; Liu, Y.; Jin, H.; Liu, Z.; Yang, W.; Yu, P.; Zhang, L.; Zhang, L. Design, synthesis and biological activities of 2,3-dihydroquinazolin-4(1H)-one derivatives as TRPM2 inhibitors. *Eur. J. Med. Chem.* **2018**, *152*, 235−252.

(4) Guo, W.; Chen, L. Recent progress in structural studies on canonical TRP ion channels. *Cell Calcium* **2019**, *83*, 102075.

(5) Wang, H.; Cheng, X.; Tian, J.; Xiao, Y.; Tian, T.; Xu, F.; Hong, X.; Zhu, M. X. TRPC channels: Structure, function, regulation and recent advances in small molecular probes. *Pharmacol. Ther.* **2020**, *209*, 107497.

(6) Huang, P.; Wang, C. Y.; Gou, S. M.; Wu, H. S.; Liu, T.; Xiong, J. X. Isolation and biological analysis of tumor stem cells from pancreatic adenocarcinoma. *World J. Gastroenterol.* **2008**, *14*, 3903−3907.

(7) Wu, X.; Eder, P.; Chang, B.; Molkentin, J. D. TRPC channels are necessary mediators of pathologic cardiac hypertrophy. *Proc. Natl. Acad. Sci. U. S. A.* **2010**, *107*, 7000−7005.

(8) Tauseef, M.; Knezevic, N.; Chava, K. R.; Smith, M.; Sukriti, S.; Gianaris, N.; Obukhov, A. G.; Vogel, S. M.; Schraufnagel, D. E.; Dietrich, A.; Birnbaumer, L.; Malik, A. B.; Mehta, D. TLR4 activation of TRPC6-dependent calcium signaling mediates endotoxin-induced lung vascular permeability and inflammation. *J. Exp. Med.* **2012**, *209*, 1953−1968.

(9) Dietrich, A.; Mederos, Y. S. M.; Gollasch, M.; Gross, V.; Storch, U.; Dubrovska, G.; Obst, M.; Yildirim, E.; Salanova, B.; Kalwa, H.; Essin, K.; Pinkenburg, O.; Luft, F. C.; Gudermann, T.; Birnbaumer, L. Increased vascular smooth muscle contractility in TRPC6−/− mice. *Mol. Cell. Biol.* **2005**, *25*, 6980−6989.
(10) Su, Y.; Chen, Q.; Ju, Y.; Li, W.; Li, W. Palmitate induces human glomerular mesangial cells fibrosis through CD36-mediated transient receptor potential canonical channel 6/nuclear factor of activated T cell 2 activation. *Biochim. Biophys. Acta, Mol. Cell Biol. Lipids* **2020**, *1865*, 158793.
(11) Lin, B. L.; Matera, D.; Doerner, J. F.; Zheng, N.; Del Camino, D.; Mishra, S.; Bian, H.; Zeveleva, S.; Zhen, X.; Blair, N. T.; Chong, J. A.; Hessler, D. P.; Bedja, D.; Zhu, G.; Muller, G. K.; Ranek, M. J.; Pantages, L.; McFarland, M.; Netherton, M. R.; Berry, A.; Wong, D.; Rast, G.; Qian, H. S.; Weldon, S. M.; Kuo, J. J.; Sauer, A.; Sarko, C.; Moran, M. M.; Kass, D. A.; Pullen, S. S. In vivo selective inhibition of TRPC6 by antagonist BI 749327 ameliorates fibrosis and dysfunction in cardiac and renal disease. *Proc. Natl. Acad. Sci. U. S. A.* **2019**, *116*, 10156−10161.
(12) Li, Y.; Jia, Y. C.; Cui, K.; Li, N.; Zheng, Z. Y.; Wang, Y. Z.; Yuan, X. B. Essential role of TRPC channels in the guidance of nerve growth cones by brain-derived neurotrophic factor. *Nature* **2005**, *434*, 894−898.
(13) Paez Espinosa, E. V.; Murad, J. P.; Ting, H. J.; Khasawneh, F. T. Mouse transient receptor potential channel 6: role in hemostasis and thrombogenesis. *Biochem. Biophys. Res. Commun.* **2012**, *417*, 853−856.
(14) Cai, R.; Ding, X.; Zhou, K.; Shi, Y.; Ge, R.; Ren, G.; Jin, Y.; Wang, Y. Blockade of TRPC6 channels induced G2/M phase arrest and suppressed growth in human gastric cancer cells. *Int. J. Cancer* **2009**, *125*, 2281−2287.
(15) Aydar, E.; Yeo, S.; Djamgoz, M.; Palmer, C. Abnormal expression, localization and interaction of canonical transient receptor potential ion channels in human breast cancer cell lines and tissues: a potential target for breast cancer diagnosis and therapy. *Cancer Cell Int.* **2009**, *9*, 23.
(16) Ding, X.; He, Z.; Zhou, K.; Cheng, J.; Yao, H.; Lu, D.; Cai, R.; Jin, Y.; Dong, B.; Xu, Y.; Wang, Y. Essential role of TRPC6 channels in G2/M phase transition and development of human glioma. *J. Natl. Cancer Inst.* **2010**, *102*, 1052−1068.
(17) El Boustany, C.; Bidaux, G.; Enfissi, A.; Delcourt, P.; Prevarskaya, N.; Capiod, T. Capacitative calcium entry and transient receptor potential canonical 6 expression control human hepatoma cell proliferation. *Hepatology* **2008**, *47*, 2068−2077.
(18) Ding, X.; He, Z.; Shi, Y.; Wang, Q.; Wang, Y. Targeting TRPC6 channels in oesophageal carcinoma growth. *Expert Opin. Ther. Targets* **2010**, *14*, 513−527.
(19) Urban, N.; Hill, K.; Wang, L.; Kuebler, W. M.; Schaefer, M. Novel pharmacological TRPC inhibitors block hypoxia-induced vasoconstriction. *Cell Calcium* **2012**, *51*, 194−206.
(20) Li, W.; Chen, X.; Riley, A. M.; Hiett, S. C.; Temm, C. J.; Beli, E.; Long, X.; Chakraborty, S.; Alloosh, M.; White, F. A.; Grant, M. B.; Sturek, M.; Obukhov, A. G. Long-term spironolactone treatment reduces coronary TRPC expression, vasoconstriction, and atherosclerosis in metabolic syndrome pigs. *Basic Res. Cardiol.* **2017**, *112*, 54.
(21) Bernichtein, S.; Pigat, N.; Barry Delongchamps, N.; Boutillon, F.; Verkarre, V.; Camparo, P.; Reyes-Gomez, E.; Mejean, A.; Oudard, S. M.; Lepicard, E. M.; Viltard, M.; Souberbielle, J.-C.; Friedlander, G.; Capiod, T.; Goffin, V. Vitamin D3 Prevents Calcium-Induced Progression of Early-Stage Prostate Tumors by Counteracting TRPC6 and Calcium Sensing Receptor Upregulation. *Cancer Res.* **2017**, *77*, 355−365.
(22) Urban, N.; Wang, L.; Kwiek, S.; Rademann, J.; Kuebler, W. M.; Schaefer, M. Identification and Validation of Larixyl Acetate as a Potent TRPC6 Inhibitor. *Mol. Pharmacol.* **2016**, *89*, 197−213.
(23) Diez-Bello, R.; Jardin, I.; Lopez, J. J.; El Haouari, M.; Ortega-Vidal, J.; Altarejos, J.; Salido, G. M.; Salido, S.; Rosado, J. A. (−)Oleocanthal inhibits proliferation and migration by modulating Ca(2+) entry through TRPC6 in breast cancer cells. *Biochim. Biophys. Acta, Mol. Cell Res.* **2019**, *1866*, 474−485.
(24) Zhou, B.; Wang, Y.; Zhang, C.; Yang, G.; Zhang, F.; Yu, B.; Chai, C.; Cao, Z. Ribemansides A and B, TRPC6 Inhibitors from Ribes manshuricum That Suppress TGF-β1-Induced Fibrogenesis in HK-2 Cells. *J. Nat. Prod.* **2018**, *81*, 913−917.
(25) Chen, R. C.; Sun, G. B.; Ye, J. X.; Wang, J.; Zhang, M. D.; Sun, X. B. Salvianolic acid B attenuates doxorubicin-induced ER stress by inhibiting TRPC3 and TRPC6 mediated Ca(2+) overload in rat cardiomyocytes. *Toxicol. Lett.* **2017**, *276*, 21−30.
(26) Merritt, J. E.; Armstrong, W. P.; Benham, C. D.; Hallam, T. J.; Jacob, R.; Jaxa-Chamiec, A.; Leigh, B. K.; McCarthy, S. A.; Moores, K. E.; Rink, T. J. SK&F 96365, a novel inhibitor of receptor-mediated calcium entry. *Biochem. J.* **1990**, *271*, 515−522.
(27) Inoue, R.; Okada, T.; Onoue, H.; Hara, Y.; Shimizu, S.; Naitoh, S.; Ito, Y.; Mori, Y. The transient receptor potential protein homologue TRP6 is the essential component of vascular alpha(1)-adrenoceptor-activated Ca(2+)-permeable cation channel. *Circ. Res.* **2001**, *88*, 325−332.
(28) Maier, T.; Follmann, M.; Hessler, G.; Kleemann, H.-W.; Hachtel, S.; Fuchs, B.; Weissmann, N.; Linz, W.; Schmidt, T.; Lohn, M.; Schroeter, K.; Wang, L.; Rütten, H.; Stübing, C. Discovery and pharmacological characterization of a novel potent inhibitor of diacylglycerol-sensitive TRPC cation channels. *Br. J. Pharmacol.* **2015**, *172*, 3650−3660.
(29) Motoyama, K.; Nagata, T.; Kobayashi, J.; Nakamura, A.; Miyoshi, N.; Kazui, M.; Sakurai, K.; Sakakura, T. Discovery of a bicyclo[4.3.0]nonane derivative DS88790512 as a potent, selective, and orally bioavailable blocker of transient receptor potential canonical 6 (TRPC6). *Bioorg. Med. Chem. Lett.* **2018**, *28*, 2222−2227.
(30) Häfner, S.; Burg, F.; Kannler, M.; Urban, N.; Mayer, P.; Dietrich, A.; Trauner, D.; Broichhagen, J.; Schaefer, M. A (+)-Larixol Congener with High Affinity and Subtype Selectivity toward TRPC6. *ChemMedChem* **2018**, *13*, 1028−1035.
(31) Bai, Y.; Yu, X.; Chen, H.; Horne, D.; White, R.; Wu, X.; Lee, P.; Gu, Y.; Ghimire-Rijal, S.; Lin, D. C.-H.; Huang, X. Structural basis for pharmacological modulation of the TRPC6 channel. *eLife* **2020**, *9*, No. e53311.
(32) Qu, C.; Ding, M.; Zhu, Y.; Lu, Y.; Du, J.; Miller, M.; Tian, J.; Zhu, J.; Xu, J.; Wen, M.; Er-Bu, A.; Wang, J.; Xiao, Y.; Wu, M.; McManus, O. B.; Li, M.; Wu, J.; Luo, H. R.; Cao, Z.; Shen, B.; Wang, H.; Zhu, M. X.; Hong, X. Pyrazolopyrimidines as Potent Stimulators for Transient Receptor Potential Canonical 3/6/7 Channels. *J. Med. Chem.* **2017**, *60*, 4680−4692.
(33) Ding, M.; Wang, H.; Qu, C.; Xu, F.; Zhu, Y.; Lv, G.; Lu, Y.; Zhou, Q.; Zhou, H.; Zeng, X.; Zhang, J.; Yan, C.; Lin, J.; Luo, H. R.; Deng, Z.; Xiao, Y.; Tian, J.; Zhu, M. X.; Hong, X. Pyrazolo[1,5-a]pyrimidine TRPC6 antagonists for the treatment of gastric cancer. *Cancer Lett.* **2018**, *432*, 47−55.

https://doi.org/10.1021/acsomega.1c00514
ACS Omega 2021, 6, 9196−9203